Theoretical and Experimental Evaluation of the Influence of the Length of Drill Rods in the SPT-T Test

Anna Silvia Palcheco Peixoto, Luttgardes de Oliveira Neto, Valéria Borin Antenor

Abstract. The influence of soil drill rod length on the *N* value in the SPT-T test has been studied extensively by Mello (1971), Schmertmann & Palacios (1979), Odebrecht *et al.* (2002) and Cavalcante (2002). This paper presents an analysis of the Standard Penetration Test supplemented with torque measurement (SPT-T). A theoretical study of the resistance of the rod material to torsion and bending indicated that the shear stress caused by the rod self-weight represents less than 1% of that caused by the torsional moment. An experimental study with electric torquemeters attached to a horizontal rod system, as well as two field tests in the vertical direction, were also carried out to compare and substantiate the results. The purpose of these tests was to analyze changes along the length of the rod in response to successive increments at 1-meter intervals. Torque measurements were taken at each increment of the length to ascertain the accuracy of the theoretical data. The difference between the applied torque and the measured torque at the end of rod system was lower than the minimum scale of mechanical torquemeters used in practice.

Keywords: SPT-T, torque measurement, torquemeter, rod length.

1. Introduction

The standard penetration test (SPT) is commonly used in the design of pile and shallow foundations in Brazilian foundation construction practices. Mayne (2001), who questioned the notion that just one number (an N-value) suffices to estimate a wide range of soil parameters, recommended the use of *in situ* testing with hybrid devices. Ranzini (1988) proposed supplementing the conventional SPT test with torque measurements required to turn the split-spoon sampler after driving.

A simple test can be performed by drilling, following the Brazilian ABNT NBR 6484 (2001) standard. After penetration of the split-spoon sampler, keeping count of the hammer blows, an adapter is attached to the anvil, onto which the torquemeter is attached. A centralizing device should be placed either on the top of the hole or inside the pipe to prevent the rod from shifting off-center in the hole during the application of torque. The rod-sampler set is then turned, using the torquemeter. The maximum torque is measured and turning continues to be applied until the torque remains constant, at which point the residual torque value is determined.

Torque is measured at the top of the rod-sampler system, Fig. 1a, but friction, as proposed by Ranzini (1994), is calculated considering only adhesion at the sampler-soil interface, Eq. (1):

$$f_T = \frac{T}{(41.336 \times h - 0.032)} \quad (1)$$

where f_T is sampler-soil adhesion, kPa; T is the measured torque, kN.m; and h is the depth of penetration of the sampler, m.

The constants in this equation are based on sample dimensions. In this paper, the Raymond split-spoon sampler is considered (ABNT NBR 6484-2001).

The influence of rod length on the torque measurements should be checked, since the readings are taken at the upper end of the sampler-rod system, while the actual load is borne by the sampler. This paper describes the first study in which the rod system is considered in a horizontal position (Fig. 1b) to allow for control of the applied torque. The experimental findings are preceded by a theoretical study of simple torsion, bending and bending-torsion concepts in a thin-walled tubular steel shaft.

Electric torquemeters designed by Peixoto (2001) were used here. These torquemeters were equipped with a data acquisition system coupled to a horizontal rod system to control the applied torque, Fig. 1b. The purpose of these tests was to analyze 1-meter to 20-meter long rods, with the torque measured at the ends of the rod system to ensure the accuracy of the data.

The SPT-T tests were carried out vertically, but experimental loading must be done with the rods in the horizontal position to allow for control of the applied torque, since the results of field tests depend on soil resistance. Moreover, field tests enable one to evaluate how and to what extent the rod's instability affects the accuracy of the SPT-T test.

The theoretical study that preceded the experimental tests was fundamental in understanding the behavior of

Anna Silvia Palcheco Peixoto, D.Sc., Assistant Professor, Departamento de Engenharia Civil, Faculdade de Engehraria, Universidade Estadual Paulista, Bauru, SP, Brazil. e-mail: anna@feb.unesp.br.
Luttgardes de Oliveira Neto, D.Sc., Assistant Professor, Departamento Engenharia Civil, Faculdade de Engenharia, Universidade Estadual Paulista, Bauru, SP, Brazil. e-mail: lutt@feb.unesp.br.
Valéria Borin Antenor, Civil Engineer, Consórcio Queiroz Galvão/Odebrecht, São Paulo, SP, Brazil. e-mail: valeria_antenor@hotmail.com.
Submitted on January 30, 2008; Final Acceptance on July 17, 2009; Discussion open until September 30, 2010.

rods during the SPT-T test, clarifying the difference between the torque applied at the upper part of the rod system and the torque at the sampler-soil interface.

2. Methodology

The present study aimed to determine the influence of rod length on the *N* value in the SPT-T test. Therefore, a theoretical study was first made to provide the necessary background for analyzing soil drill rod behavior, in order to gain a better understanding of how experimental tests are performed in practical engineering.

2.1. Theoretical background

Concepts of materials resistance and buckling phenomena are necessary for theoretical analyses and comparisons with experimental results.

Based on the concept of free torsion (or uniform torsion) as a type of load in which all the cross sections of a rod are loaded only by a torsional moment, any other kind of internal load such as the bending moment, normal load or shear load is equal to zero. An initial hypothesis is that the cross sections undergo free warping, but their projections remain undeformed. This phenomenon does not occur with *in situ* SPT test rods that have a circular thin-walled section.

However, in the initial phase of this research, which was conducted in the laboratory, thin-walled section rods were subjected to normal stresses caused only by the bending moment. The rods were placed in a horizontal position and loaded with metal weights, as illustrated in Fig. 1b. The diagram in Fig. 2 depicts a beam with a vertical load P and its respective load diagrams.

In the second phase, which consisted of field tests, the rods were positioned vertically and the buckling phenomenon was examined, which occurs when a structure is subjected to the action of external compression and bending. According to Schiel (1984), this phenomenon is not a problem of structural strength. The factor that determines whether the structure will be subjected to this phenomenon is its cross section dimensions (elastic buckling).

Elastic buckling is determined by analyzing the phenomenon in an axially compressed prismatic bar, as shown in Fig. 3. In this figure, the deformation of the bar is represented by the elastic curve, with the y axis representing the displacement of the cross section.

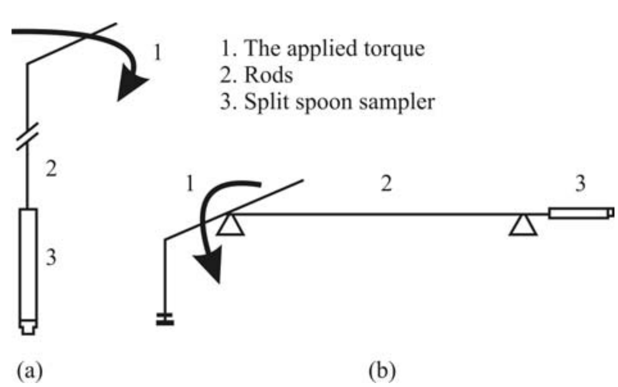

Figure 1 - (a): SPT-T test load; (b): Laboratory experimental load.

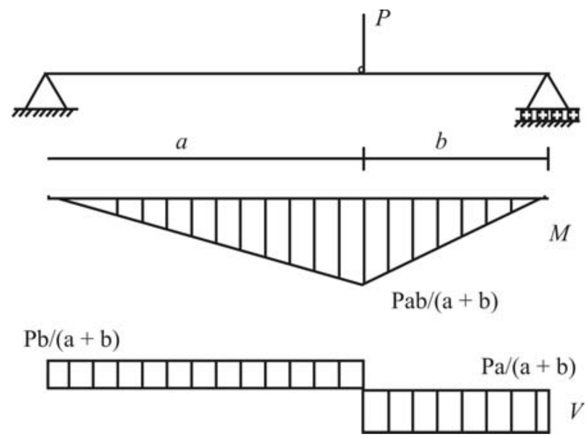

Figure 2 - Beam load diagrams.

The critical buckling load (Euler's Load) is presented in Eq. (2),

$$\frac{\pi^2}{L^2} = \frac{P}{EI} \rightarrow P_{cri} = \frac{\pi^2 EI}{L^2} \tag{2}$$

where $L = L_{fl}$ is the critical length; I is the moment of inertia of the cross section; and E is Young's modulus.

However, the goal here is to study the influence of weight on the buckling phenomenon in a bi-jointed column, which probably best represents SPT-T rods in field tests. The real elastic deformation of the bar to meet the new boundary conditions depicted in Fig. 4 is obtained by Eq. (3),

$$y = \delta \sin\left(\frac{\pi x}{L}\right) \tag{3}$$

which results in

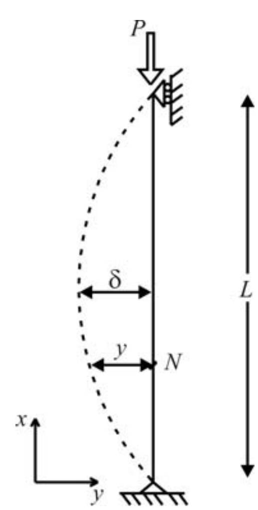

Figure 3 - Static scheme of axially compressed bar.

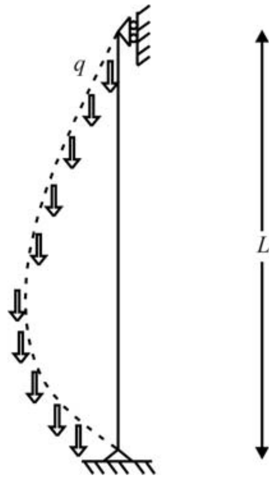

Figure 4 - Probable deformation of a bi-jointed column under its own weight.

Figure 5 - Strain gauges attached to the rod.

$$\left\{\{q \to 0.\}, \left\{q \to \frac{61.661 EI}{L^3}\right\}\right\} \quad (4)$$

where q represents the Critical Distributed Buckling Load.

Mathematica (Wolfram, 2003) software was used to solve the equation that theoretically determines the critical rod length.

To verify the theoretical calculation of the Euler load experimentally, a 2-meter length rod used in the SPT-T test was subjected to an axial compression test in the Structures Laboratory, School of Engineering, São Paulo State University, Bauru City, Brazil.

The rod was placed in a metallic frame and loaded, using a load cell and a hydraulic jack, ensuring that the ultimate buckling load would not be reached. The hydraulic jack was connected to the load cell and a data acquisition system was used to control the applied load and record the strain values.

Four strain gauges were attached vertically around the rod section at mid-length, which is the critical area for the occurrence of maximum deformations, Fig. 5.

Figure 6a shows the strain gauge arrangement, while Fig. 6b illustrates a strain gauge attached to the rod. This test was conducted to confirm Euler's critical load, since a test that could analyze only the rod's self-weight could not be performed.

2.2. Laboratory tests

The influence of length rod on the buckling phenomenon was studied using the SPT device recommended by the Brazilian NBR6484 (2001) standard. The theoretical weight of the rod was 32 N/m, its external diameter was 33.4 mm ± 2.5 mm, and its internal diameter was 24.3 mm ± 5 mm.

The laboratory tests were performed to control the applied torque without soil resistance. The calibration system

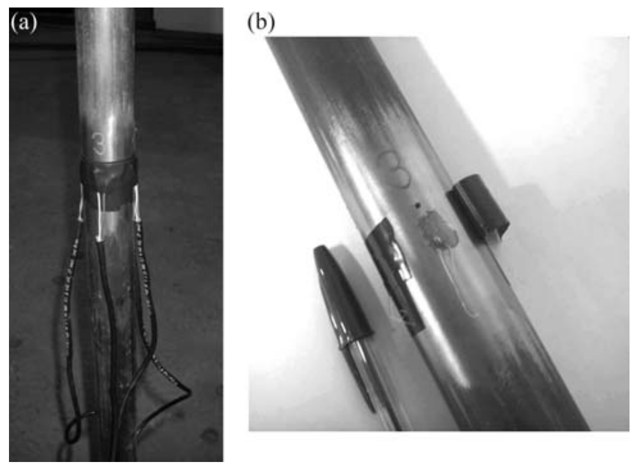

Figure 6 - Strain gauge details.

represents the field operator applying the torque, but with the rods in a horizontal position, as illustrated in Fig. 7. The results were recorded by two electric torquemeters positioned at the extremities of the rod system.

The rods were positioned horizontally and their length varied from 1 m to 20 m. Tripods equipped with roller bearings were used to reduce the friction between the rods and tripods, Fig. 8.

2.3. Field tests

The purpose of the field tests was to verify the influence of rod length on practical SPT-T tests. These tests were performed in winter (July 2006) at the Experimental Foundation Site, School of Engineering, São Paulo State University, Bauru City, São Paulo State, Brazil, Fig. 9.

Two different tests were carried out. The first was in a borehole, as performed in a standard SPT test, while the second one was carried out inside a pit with a diameter of 0.80 m, in which it was possible to execute a test similar to

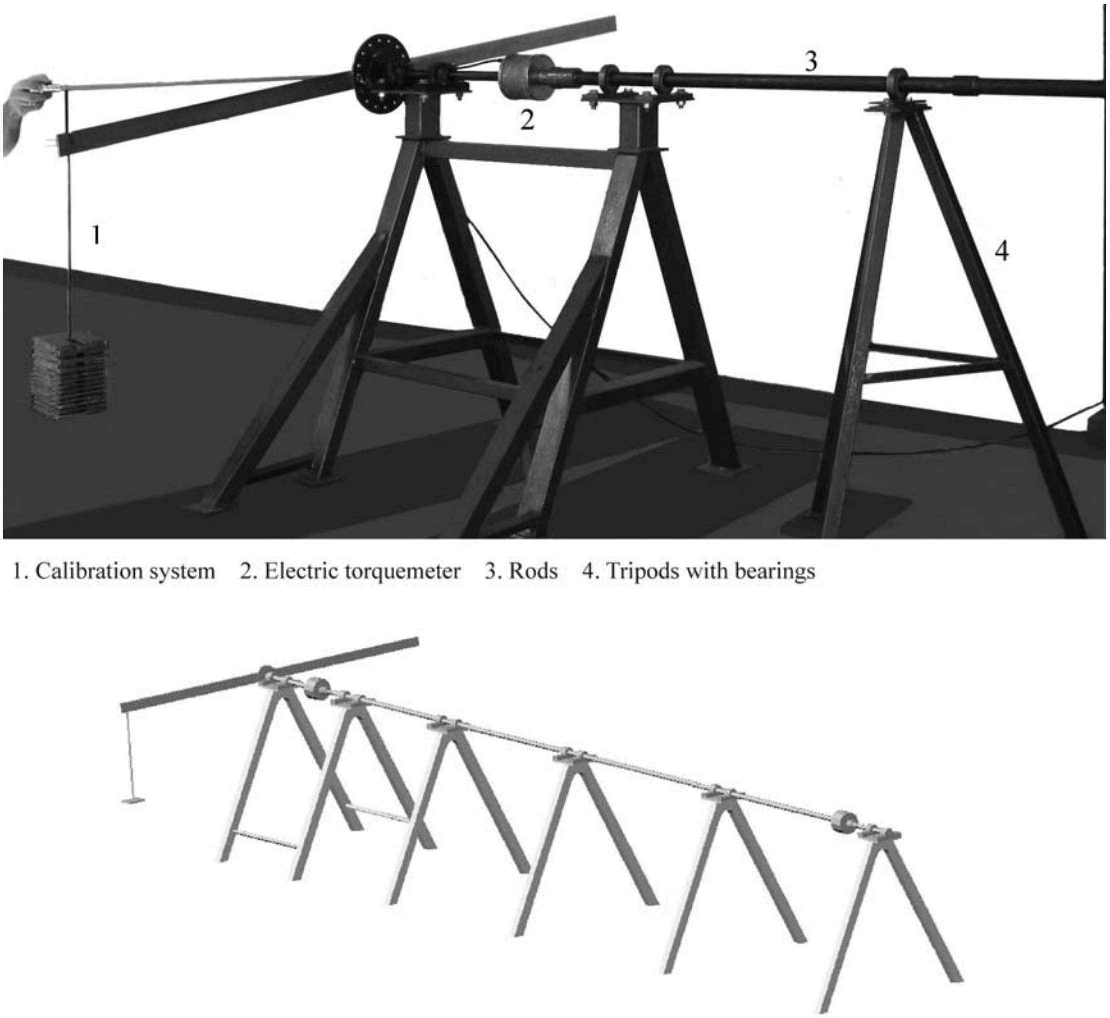

Figure 7 - Rod system.

Figure 8 - Roller bearing.

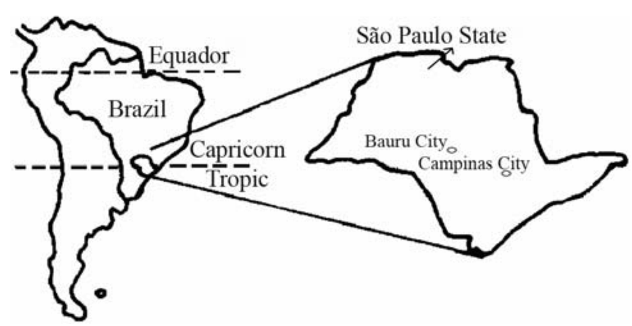

Figure 9 - Site location.

the laboratory test, *i.e.*, using two electric torquemeters, the first attached to the upper end of the rod system and the second between the sampler and the rod system.

Figure 10 illustrates the two test configurations, including previous *in situ* tests carried out in this area.

3. Results and Analysis

This analysis is essential, since rod instability may impair the practical results. The presentation of this analysis is followed by an analysis of the laboratory and field tests.

3.1. Theoretical analyses

In the static scheme, Fig. 11, the rod's self-weight is considered as a transversally distributed load (q = 32 N/m) and the applied torsion moment, M_t = 500 N.m, is greater

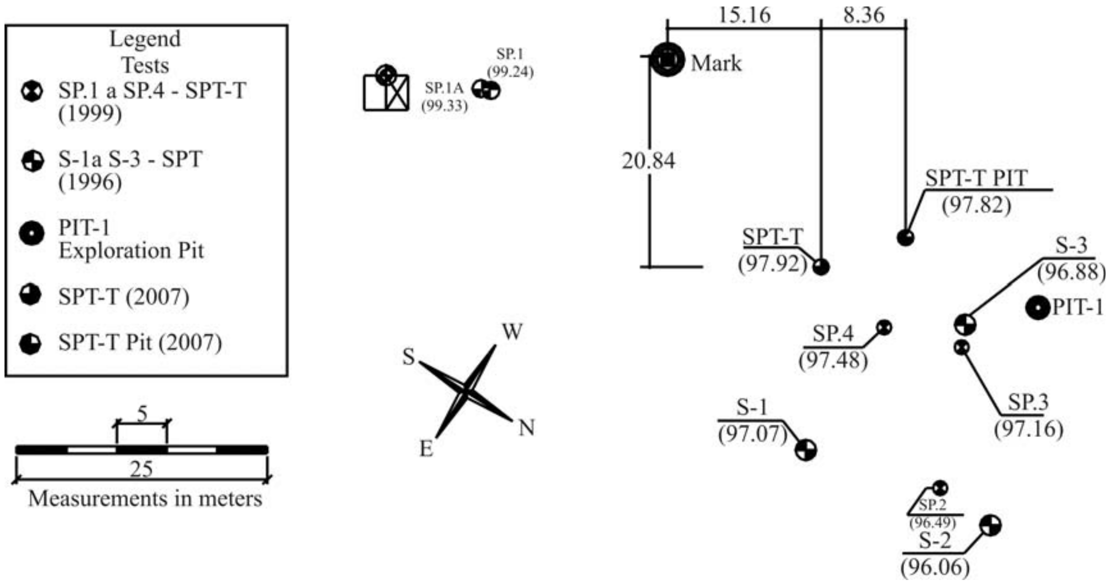

Figure 10 - Configuration of the tests conducted at the Experimental Foundation Site of UNESP's Faculty of Engineering at Bauru.

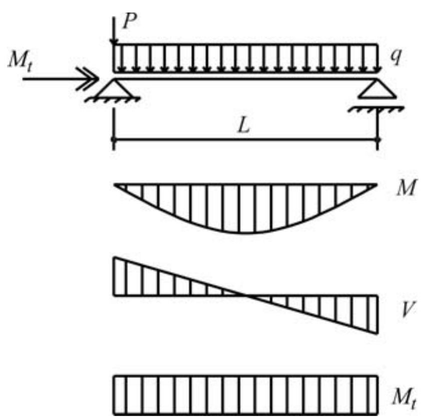

Figure 11 - Static scheme showing the rod's self-weight load and torsion moment.

Table 1 - Cross section dimensions and properties.

d_{in} (m)[1]	d_{out} (m)[2]	d_m (m)[3]
$2.390.10^{-2}$	$3.355.10^{-2}$	$2.8725.10^{-2}$
A_{cross} (m^2)[4]	t (m)[5]	A_m.(m^2)[6]
$4.3542.10^{-2}$	$4.8250.10^{-3}$	$6.4805.10^{-4}$
I_t (m^4)[7]	I (m^4)[8]	r (cm)[9]
$1.089.10^{-4}$	$7.3034.10^{-8}$	1.030

[1]Internal diameter; [2]External diameter; [3]Medium diameter; [4]Cross section area; [5]Cross section thickness; [6]Area enclosed by the medium curve; [7]Torsion inertial momentum; [8]Bending inertial momentum; [9]Radius of gyration.

Table 2 - General stress.

τ_V (MPa)[1]	τ_{Mt} (MPa)[2]	σ (MPa)[6]
$7.35.10^{-1}$	79.95	0.82

[1]Bending shear stress; [2]Torsion shear stress at cross section; [6]Bending stress.

than the usual field test loads. The rod's geometric properties are listed in Table 1.

As can be seen in Table 2, the shear stress (τ_V) caused by bending was less than 1% of the shear stress caused by the torsional moment, τ_{Mt}, Eq. (5), since it is 20 m long in the rod system.

$$\tau_{Mt} = \frac{M_t}{2tA_m} \tag{5}$$

where τ_{Mt} is the torsion shear stress at the cross section, MPa; t is the cross section thickness, m; and A_m is the area enclosed by the medium curve, m^2.

3.1.1. Buckling

Based on the theoretical expressions, Table 4 illustrates the critical load results for the columns with articulated ends. The Critical Buckling Load (Euler load), P_{cri}, is obtained by Eq. (2) and the Critical (Self-Weight) Distributed Buckling Load, q_{cri}, is obtained by Eq. (4). The Equivalent Critical Load ($P_{cri,eq}$) is calculated by multiplying the Critical Self-Weight Buckling Load (q_{cri}) by the corresponding rod length (L). It is then possible to compare those values with the theoretical Critical Buckling Load (P_{cri}, far right column, Table 4).

Since the rod's weight is 32 N/m, note that the *self-weight* is not a limiting factor for the occurrence of buckling up to 20 m (as shown in the q_{cri} column, Table 4). These results indicate that the influence of the column's

Table 3 - Shear stress caused by bending (τ_V) and torsional (τ_{Mt}) moments.

L (m)	V (N)	τ_V (MPa)	τ_{Mt} (MPa)	$\frac{\tau_V}{\tau_{Mt}}$(%)
1	16	0.037	79.95	0.046
5	80	0.184	79.95	0.230
10	160	0.367	79.95	0.460
15	240	0.551	79.95	0.689
20	320	0.735	79.95	0.919

self-weight does not affect the buckling phenomenon in the STT-T test.

Even admitting, hypothetically, that the weight of the SPT operator with a magnitude of 772.1 N (column 4, Table 4) is applied axially to the upper extremity of the rod during the *in situ* test, this would be considered a critical load for a rod with over 11 m of free length. Considering depths of more than 11 m, this influence may cause lateral instability of the rod system, given that critical loads diminish.

Table 4 - Critical Buckling Load q_{cri} as a function of the rods' length.

Length L (m)	Critical self-weight buckling load q_{cri} (N/m), Eq. (4)	Equivalent critical load $P_{cri,eq}$ (N)	Critical buckling load (Euler load) P_{cri} (N), Eq. (2)
1	583706.3	583706.3	93423.0
2	72963.3	145926.6	23355.7
3	21618.8	64856.3	10380.3
4	9120.4	36481.6	5838.9
5	4669.7	23348.3	3736.9
6	2702.3	16214.0	2595.1
7	1701.8	11912.4	1906.6
8	1140.1	9120.4	1459.7
9	800.7	7206.2	1153.4
10	583.7	5837.1	934.2
11	438.6	4824.1	772.1
12	337.8	4053.5	648.8
13	265.7	3453.8	552.8
14	212.7	2978.1	476.7
15	173.0	2594.3	415.2
16	142.5	2280.2	364.9
17	118.8	2019.8	323.3
18	100.1	1801.6	288.3
19	85.1	1616.9	258.8
20	73.0	1459.2	233.6

It is also possible to conclude that the self-weight is less critical than the axial load the operator applies at the upper extremity of the rod. Therefore, the column's slenderness must be taken into account when defining a safety limit for the rod's free length in order to ensure the good performance of the SPT-T, considering an axially compressed column.

Table 5 shows the slenderness (λ) of the rod column calculated as a function of length and obtained by the ratio of the buckling length (L) to the radius of gyration (r).

According to the Brazilian ABNT NBR 8800/1986 code, the maximum admissible slenderness of a prismatic steel bar subjected to axial compression is 200. Considering the results found in Table 5, the critical buckling length in the rod column test is 2 m (λ = 194,2). This means that in tests conducted at deeper depths, intermediary spacers must be added at 2-meter intervals to satisfy the slenderness limit. The goal is to diminish the rod's free length, avoiding buckling and large lateral displacements of the rod column, thereby improving the efficiency of the test.

Figure 12 depicts the instant when buckling occurs in a compressed rod under the application of the critical load. The cross section at mid-span shows the maximum transversal displacement.

Considering $L_{fl} = L/\sqrt{2} = 0.7L$ for a joint-clamp bar scheme according to the ABNT NBR 8800/86 standard, it is possible to estimate the buckling load. Based on theoretical calculations (Eq. (11)), the buckling load was 46 kN. Figure 13 depicts the load *vs.* time curve obtained during the buckling test, showing a maximum load of 48.5 kN was obtained, which means a difference of about 5% over the expected value.

An analysis of Fig. 14 reveals that when the buckling load was almost attained, two pairs of the four strain gauges exhibited major deformations, distension and contraction.

Table 5 - Slenderness as a function of length.

Length (m)	λ	Length (m)	λ
1.0	97.1	11.0	1068.1
2.0	194.2	12.0	1165.2
3.0	291.3	13.0	1262.3
4.0	388.4	14.0	1359.4
5.0	485.5	15.0	1456.5
6.0	582.6	16.0	1553.6
7.0	679.7	17.0	1650.8
8.0	776.8	18.0	1747.9
9.0	873.9	19.0	1845.0
10.0	971.0	20.0	1942.1

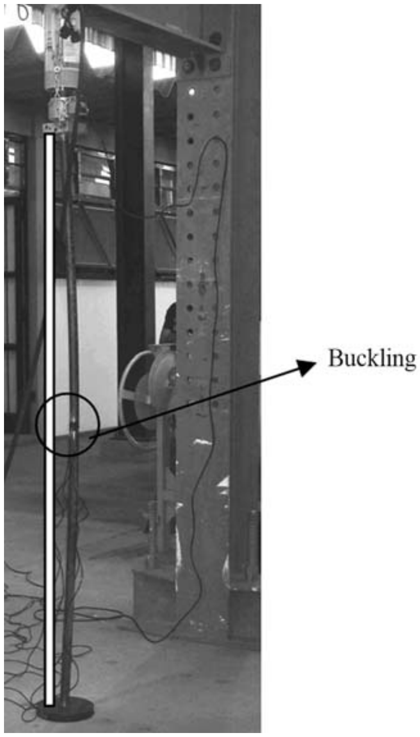

Figure 12 - Instant when buckling occurred.

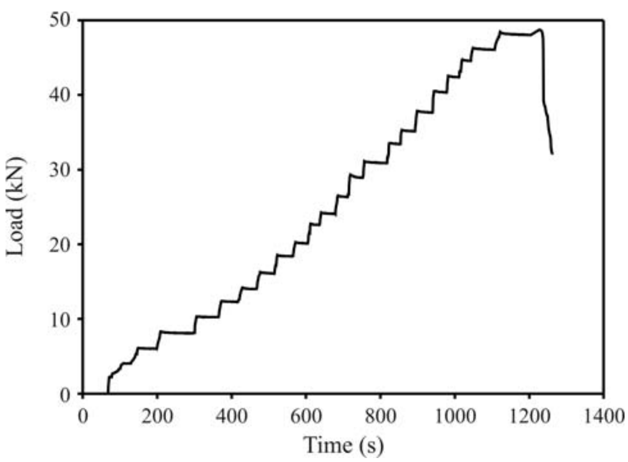

Figure 13 - Load *vs.* time curve.

3.2. Laboratory tests

The two graphs below display the values of torque obtained at the extremity close to the point where torque was applied, and the differences between the first and second torque values. In Fig. 15, the ordinate axis represents the ratio between the torque applied at the beginning (T_b) and the torque received at the end of rod system (T_e). The ordinate axis in Fig. 16 shows the values of the differences between the two torquemeters. Note that although the applied torque increases the ratio between the applied torque and the received torque, the minimum value remains constant (Fig. 15).

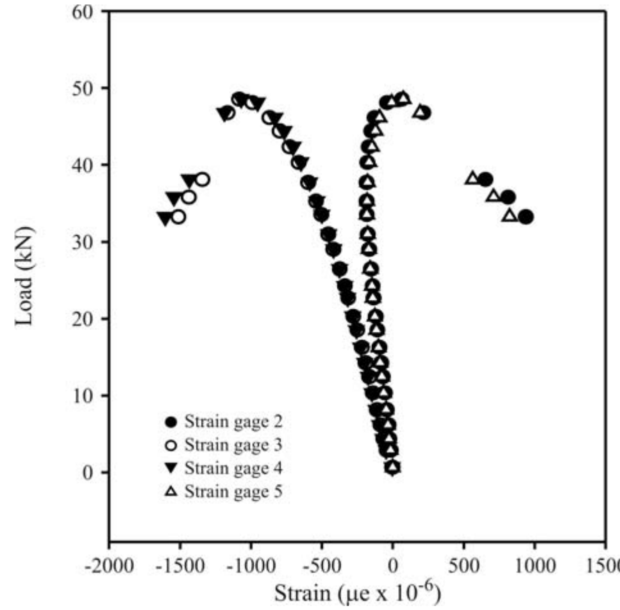

Figure 14 - Strain *vs.* load.

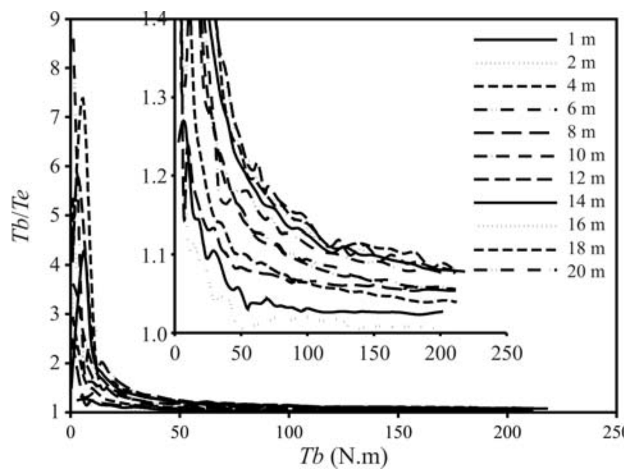

Figure 15 - *Tb*/*Te* analysis.

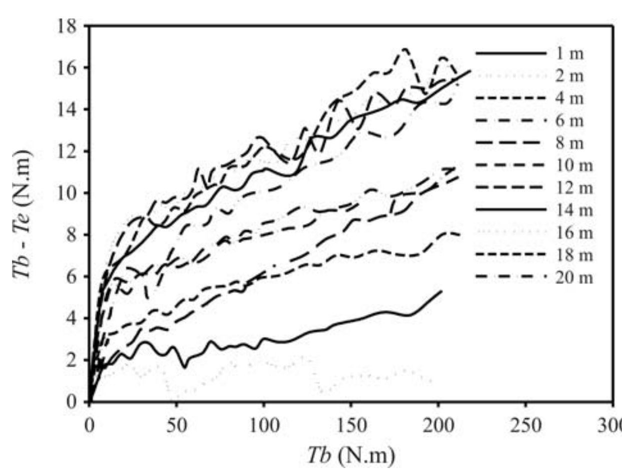

Figure 16 - (*Tb* - *Te*) *vs. Tb*.

3.3. Field tests

Figure 17 depicts the data recorded by the data acquisition system, showing the torque values from both torquemeters and the substantial differences between those values.

Table 6 lists the maximum torques recorded by the torquemeters used in the field tests. As can be observed, the differences between the two values, T_b and T_e, (on average around 16 N.m) are below the normal minimum torquemeter scale (20 N.m). These results confirm the data obtained in the laboratory tests.

4. Conclusions

Based on the laboratory and field tests, it is possible to ensure that the torque difference through rod length is lower than the minimum scale of mechanical torquemeters that are used on practical engineering (20 N.m). That way, the influence of the drill rod length is not significant considering the practical results.

Following the theoretical analyses, it can be concluded that the rod's self-weight is not the limiting factor for the buckling phenomenon. The most important rod characteristic is the column's slenderness in order to preserve the rods' stability during field tests.

As stated earlier herein, the column's slenderness should be kept to the 200 limit, which corresponds to two

Table 6 - Differences in the applied torques recorded by the two torquemeters.

Rod length (m)	Depth (m)	T_b (N.m)	T_e (N.m)	T_b - T_e (N.m)
2	1	50.2	36.9	13.3
3	2	60.2	57.6	2.6
4	3	57.7	42.6	15.1
5	4	96.8	78.9	17.9
6	5	98.6	80.7	17.9
7	6	158.7	146.4	12.3
8	7	99.5	81.2	18.3
9	8	289.9	272.0	17.9
10	9	192.9	164.2	28.7
16	15	290.7	273.2	17.5
		Average (N.m)		16.2

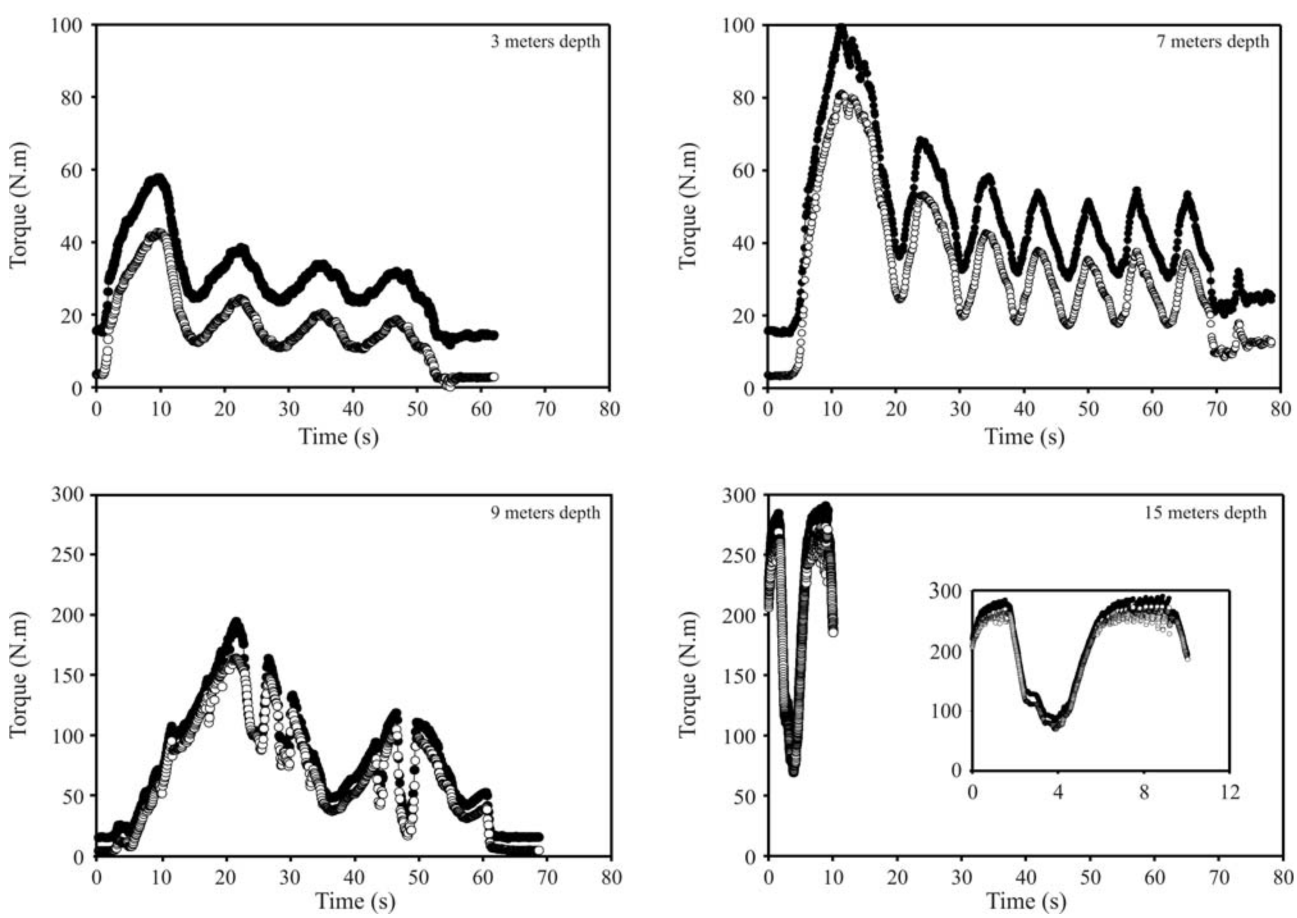

Figure 17 - Torque *vs.* time.

meters of free rod length. Intermediate spacers should be placed along the rod's entire length to avoid free rod lengths from exceeding two meters and thereby reducing the efficiency of the test.

Moreover, with regard to the sampler's penetration in response to the falling hammer, this load can be considered to have no influence down to a depth of around 12 m. However, this dynamic effect could not be eliminated, since determining it is the goal of the test.

Some important aspects to be considered are that the real column is not bi-articulated at its extremities and also that it has eccentricities along its length, neither of which are considered in the theoretical formulation. All the above described details confirm the idea that the rod's free length should be diminished by using intermediate spacers.

Acknowledgments

The authors acknowledge the financial support of the Brazilian research funding agency FAPESP (Fundação de Amparo à Pesquisa do Estado de São Paulo).

References

ABNT (2001) NBR 6484 - Execução de Sondagens de Simples Reconhecimento dos Solos, 12 pp.

ABNT (1986) Projeto e Execução de Estruturas de Aço em Edifícios, NBR 8800, 198 pp.

De Mello, V.F.B. (1971) The Standard Penetration Test. Pan-American Conference on Soils Mechanics and Foundation Engineering, Porto Rico, v. 1. 86 pp.

Cavalcante, E.H.; Danziger F.A.B.; Danziger, B.R. & Bezerra R.L. (2002). Medida de Energia do SPT: Instrumentação para Registro de Força e de Velocidade nas Hastes. XII COBRAMSEG – Congresso Brasileiro de Mecânica dos Solos e Engenharia Geotécnica, São Paulo, v. 1, pp. 97-106.

Wolfram, S. (2003) Mathematica Book, 5 th ed. Wolfram Media, Champaign, 1464 pp.

Mayne, P.W. (2001) Strain-strenght-flow parameters from enhanced *in-situ* tests. In-Situ 2001, Bali, pp. 21-48.

Odebrecht, E.; Rocha, M.M.; Bernardes, G.P. & Schnaid, F. (2002) Medidas de energia no ensaio SPT. Proc. XII COBRAMSEG – Congresso Brasileiro de Mecânica dos Solos e Engenharia Geotécnica, São Paulo, v. 1, pp. 107-118.

Peixoto, A.S.P. (2001) Estudo do ensaio SPT-T e sua Aplicação na Prática de Engenharia de Fundações (Study of SPT-T test and its application on Foundation Engineering). PhD Thesis, Universidade Estadual de Campinas.

Ranzini, S.M.T. (1994) SPTF: 2ª parte. Soils and Rocks, v. 17:3, p. 189-190.

Ranzini, S.M.T. (1988) SPTF. Soils and Rocks, v. 11:1, p. 29-30.

Schiel, F. (1984) Introdução à Resistência dos Materiais, 3ª ed. Editora Harper & Row do Brasil Ltda, São Paulo, 395 pp.

Schmertmann, J.H. & Palacios, A. (1979) Energy Dynamics of SPT. Journal of the Geotechnical Engineering Division, v. 105:GT8 p. 909-926.

Timoshenko, S. (1981) Resistência dos Materiais, 1ª ed. Livro Técnicos e Científicos Editora S.A., Rio de Janeiro, 518 pp.